Protein Science (1996), 5:1633-1647. Cambridge University Press. Printed in the USA.

Three-dimensional structure of the complexes of ribonuclease A with 2′,5′-CpA and 3′,5′-d(CpA) in aqueous solution, as obtained by NMR and restrained molecular dynamics

CATHERINE TOIRON, CARLOS GONZÁLEZ, MARTA BRUIX, AND MANUEL RICO
Instituto de Estructura de la Materia, CSIC, Serrano 119, 28006 Madrid, Spain

(RECEIVED March 20, 1996; ACCEPTED May 14, 1996)

Abstract

The three-dimensional structure of the complexes of ribonuclease A with cytidyl-2′,5′-adenosine (2′,5′-CpA) and deoxycytidyl-3′,5′-deoxyadenosine [3′,5′-d(CpA)] in aqueous solution has been determined by ^{1}H NMR methods in combination with restrained molecular dynamics calculations. Twenty-three intermolecular NOE cross-correlations for the 3′,5′-d(CpA) complex and 19 for the 2′,5′-CpA, together with about 1,000 intramolecular NOEs assigned for each complex, were translated into distance constraints and used in the calculation. No significant changes in the global structure of the enzyme occur upon complex formation. The side chains of His 12, Thr 45, His 119, and the amide backbone group of Phe 120 are involved directly in the binding of the ligands at the active site. The conformation of the two bases is anti in the two complexes, but differs from the crystal structure in the conformation of the two sugar rings in 3′,5′-d(CpA), shown to be in the S-type region, as deduced from an analysis of couplings between the ribose protons. His 119 is found in the two complexes in only one conformation, corresponding to position A in the free protein. Side chains of Asn 67, Gln 69, Asn 71, and Glu 111 form transient hydrogen bonds with the adenine base, showing the existence of a pronounced flexibility of these enzyme side chains at the binding site of the downstream adenine. All other general features on the structures coincide clearly with those observed in the crystal state.

Keywords: binding interactions; bound nucleotide conformation; 2D NMR solution structure; 2′,5′-CpA RNase complex; 3′,5′-d(CpA) RNase complex

Bovine pancreatic ribonuclease (RNase A, EC 3.1.27.5) is a well-known enzyme and has been studied extensively by a large variety of chemical-physical methods (for reviews see Richards & Wyckoff, 1971; Blackburn & Moore, 1982; Eftink & Biltonen, 1987). From a structural point of view, RNase A has been investigated thoroughly by X-ray diffraction analysis and, as a result, a number of precise three-dimensional structures are presently available for crystals under somewhat different conditions (Borkakoti et al., 1982; Wlodawer et al., 1983, 1988; Wlodawer, 1984). On the other hand, a highly refined structure of RNase A in aqueous solution has been determined recently by NMR methods (Santoro et al., 1993).

Reprint requests to: Manuel Rico, Instituto de Estructura de la Materia, CSIC, Serrano 119, 28006 Madrid, Spain.

Abbreviations: 2′,5′-CpA, cytidyl-2′,5′-adenosine; 3′,5′-d(CpA), deoxycytidyl-3′,5′-deoxyadenosine; COSY, correlation spectroscopy; DQF-COSY, double-quantum filter-COSY; TOCSY, total correlation spectroscopy; NOESY, NOE spectroscopy; TSP, sodium 3-trimethylsilyl (2,2,3,3-2H4) propionate.

RNase A is a small (124 residues, 13.7 kDa) pyrimidine-specific ribonuclease that catalyzes the cleavage of single-stranded RNA to yield pyrimidine-2′,3′-cyclic phosphates that are subsequently hydrolized to 3′-nucleotides. A preliminary description of aminoacyl residues involved in the catalytic process was obtained from chemical modification studies and analysis of pH dependence of enzymatic activity (Findlay et al., 1962; Crestfield et al., 1963; Hirs et al., 1965). A more detailed view of the geometry of the active site was achieved by studying the complexes between RNase A and several substrate analogues. A number of complexes with mono- and dinucleotides have been studied by X-ray crystallography (Wodak et al., 1977; Pavlovsky et al., 1978; Borkakoti et al., 1983; Howlin et al., 1987; Lisgarten et al., 1993; Zegers et al., 1994), neutron diffraction (Wlodawer et al., 1983), and NMR spectroscopy (Haar et al., 1974; Hahn & Ruterjans, 1985; Hahn et al., 1985). These studies led to the identification of His 12 and His 119 as essential residues for enzymatic activity, acting, respectively, as a general base and a general acid, as well as Lys 41, which is thought to

be involved in the stabilization of the penta-coordinate phosphorous atom in the transition state. Residues Thr 45 and Phe 120 participate directly in the binding of the substrate at the active site, whereas Gln 69, Asn 71, and Glu 111 have been proposed to interact with the adenine base at the B2 subsite (Wodak et al., 1977; Fontecilla-Camps et al., 1994; Zegers et al., 1994; see de Llorens et al., 1989 for a pictorial description of subsites).

Structural studies in aqueous solution of various complexes between RNase A and mononucleotides have been conducted by NMR. In early 1D NMR works, the structural information was obtained by monitoring the resonances of $H^{\delta 2}$ and $H^{\epsilon 1}$ histidine protons of the protein as well as the H5 and H6 protons of the pyrimidine nucleotides (Haar et al., 1974). More recently, two-dimensional NMR was applied to study the 2′- and 3′-pyrimidine nucleotide complexes (Hahn & Ruterjans, 1985). Proton resonances of 21 amino acid residues were assigned and used to locate conformational changes associated to the base type (cytidine or uridine) and/or the 2′- or 3′- position of the phosphate group in the nucleotide. Once given the small number of assigned proton probes, the conclusions of these works were necessarily of a fragmentary character. More recently, solution structural studies of the complexes between RNase A and four mononucleotides (2′-CMP, 2′-UMP, 3′-CMP, and 3′-UMP) on the basis of the complete assignments of the free protein have been conducted and a preliminary report has been given (Bruix et al., 1991).

In spite of this large body of structural studies, there are still some questions that remain about the interactions of enzyme–substrate that may have a role in the processes of binding and catalysis. The two dinucleoside mono-phosphates 2′,5′-CpA and 3′,5′-d(CpA) are not substrates, but rather they serve as competitive inhibitors. However, once given their close relationship to actual substrates, the study of the structure of these complexes will necessarily provide insights into the mechanism of the transesterification reaction. Some of these open questions, related, for instance, to the residues involved in the specific binding of substrates extending beyond the active site or to which of the two alternative positions of the side chain of His 119 is the really active on the transesterification step, have ben answered by X-ray diffraction structural studies (Fontecilla-Camps et al., 1994; Zegers et al., 1994). However, results pertinent to the crystal state may not always be directly extrapolable to the solution state, so the derived structural features must be tested by studying the structure of the complexes in aqueous solution. This is the main objective of this work, in which the three-dimensional structure of the complexes of RNase A with 2′,5′-CpA and 3′,5′-d(CpA) has been determined by NMR methods, with a view of obtaining meaningful conclusions about similarities and differences in the structural and dynamics of these complexes in the solution and crystal states.

Results

Standard 2D NMR methodology was used to assign the proton spectra (Wüthrich, 1986). The process was greatly facilitated by the previous assignment of the free enzyme (Rico et al., 1989; Robertson et al., 1989). The assignment of the dinucleotide resonances was mainly based on TOCSY and COSY experiments carried out with samples with a 2:1 protein:ligand ratio at pH 5.5 in D_2O. In both complexes, the sugar spin systems were identified separately by successive ^3J coupling correlations starting from the anomeric H1′ protons, which have a characteristic chemical shift in the 5.90–6.40 ppm region. Intramolecular NOEs involving H1′, H2′, and H2″ protons of the sugar rings with the base protons allowed the identification of sugar and base moieties belonging to the same nucleotide (see Figs. 1, 2). The complete list of protein and dinucleoside monophosphate proton assignments are reported in the Electronic Appendix.

Chemical shift differences between free and complexed RNase A

Most of the chemical shift variations that occur with complex formation are located in very restricted regions of the protein sequence (see Fig. 3), whose residues display relatively large chemical shift changes in their H^N and H^α resonances. Thus, the regions 8–12, 41–46, and 118–122, which are considered part of the active site, show changes in the chemical shifts of their backbone protons, as well as the regions 83–85 and 106–108, in the β-strands adjacent to it. There are some differences between the observed chemical shift variations in the two complexes. The H^N resonance in residue 20 is only affected in the 2′,5′-CpA complex, whereas the H^N resonance of residues 80 and 122 are significantly shifted in the 3′,5′-d(CpA) complex only. Also, H^N chemical shift changes in the region 66–69, which is part of the adenine binding site, are larger in 3′,5′-d(CpA) complex than in the 2′,5′-CpA one.

The amide proton resonances of Thr 45 and Phe 120 deserve special attention. These two resonances are not observed in the spectra recorded at pH 5.5. In the 3′-5′d(CpA) complex, the change in the amide proton chemical shift of Phe 120 is −0.10 ppm at pH 4.0 and −0.48 ppm at pH 4.5. This differential change with pH must be attributed primarily to the change in the ionization state of the phosphodiester group when going from the mono- to the di-anionic form, which implies the involvement of this amide proton in its binding. As indicated by the change in chemical shift with the relative concentration of enzyme and ligand, the free and complexed proteins are in the fast to intermediate range of exchange on the NMR time scale. The amide proton resonance of Phe 120 at pH 5.5 must be exchange-broadened beyond detection, which can be due to a still larger value of the binding chemical shift as well as a lower value of the dissociation exchange rate. A similar effect must be operating for the amide proton of Thr 45 in both complexes.

Some side-chain protons present a large chemical shift variation with complex formation. Thus, the β-proton resonances of Ser 123 show a significant splitting [0.11 ppm in the one with 3′,5′-d(CpA) and 0.08 ppm in the one with 2′,5′-CpA], which is not present in the free enzyme. Similarly, the proton resonances of the γ-methyl groups of Val 43 show splittings of +0.15 ppm in the 3′,5′-d(CpA) complex and +0.23 ppm in the 2′,5′-CpA one, which can be related to the adoption by the side chain of a more fixed conformation around $\chi 1$ than the motional averaged one corresponding to the free enzyme. Some other proton resonances significantly affected by complexation are one of the H^βs of Cys 84 and that of the methyl group in Ala 109. Methyl protons of Val 118 and one of the H^βs of His 119 show large chemical shift differences between the two complexes. In both cases, the chemical shift variation that occurs with complex formation is larger in the 3′,5′-d(CpA).

The aromatic protons of Phe 120 and those in the side chains of His 12 and His 119 (both residues involved in the catalytic

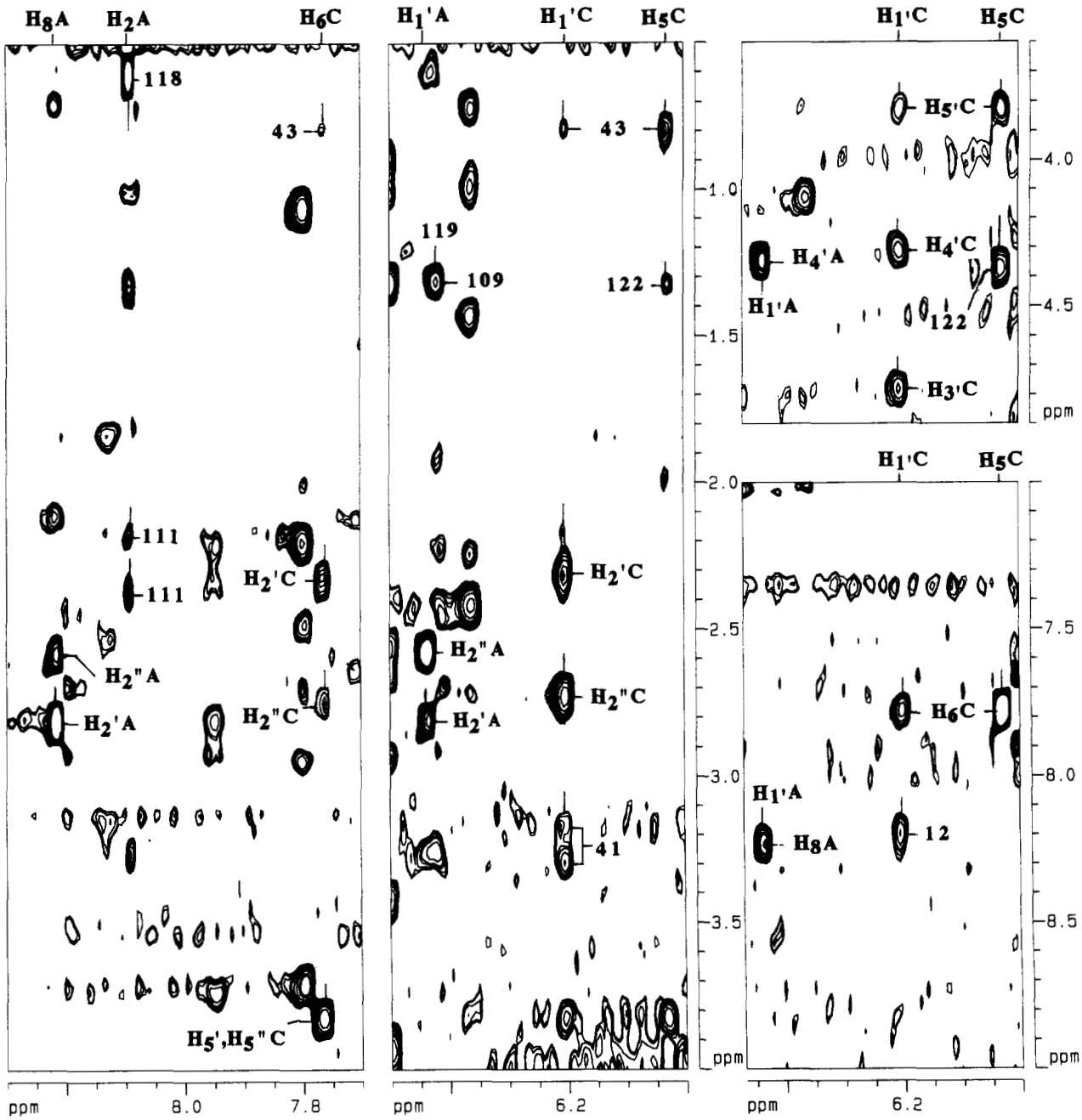

Fig. 1. Selected region of the two-dimensional NOESY spectra RNase A/3′,5′-d(CpA) 1:1 complex (4 mM, pH 5.5, 35 °C, D_2O), showing intradinucleotide NOEs and intermolecular NOEs with His 12, Lys 41, Val 43, Glu 111, Val 118, and Ala 122.

process), undergo important chemical shift variation on complexation (see Table S4 in the Electronic Appendix). Particularly important is the chemical shift variation of the resonances corresponding to the aromatic protons H^{δ} of Phe 120 [−0.32 ppm for 2′,5′-CpA complex and −0.45 ppm for 3′,5′-d(CpA) complex] and $H^{\delta 2}$ of His 119 [−0.38 ppm and −0.7 ppm for 2′,5′-CpA and 3′,5′-d(CpA)]. As discussed below, those up-field shifts must be a consequence of the pseudo-stacking found between these two aromatic side chains with the cytidine and adenine bases, respectively.

All of the above differences in chemical shifts refer to residues at the active site or in their surroundings. In contrast, most of the enzyme proton resonances are virtually unaffected upon complexation. This fact strongly indicates that the binding of these two inhibitors do not induce global conformational changes in the enzyme. Shifts observed in the vicinity of the ligand may have their origin in either conformational rearrangements of groups in the enzyme or in field effects arising from anisotropic groups of the nucleotides, mainly ring current effects from the cytidine or adenine bases. These effects have been calculated in the resulting three-dimensional structures. The ring current shifts for NH and H^{α} protons are included in the Electronic Appendix. The areas of the sequence affected by the ring currents coincide with the regions with larger chemical shift vari-

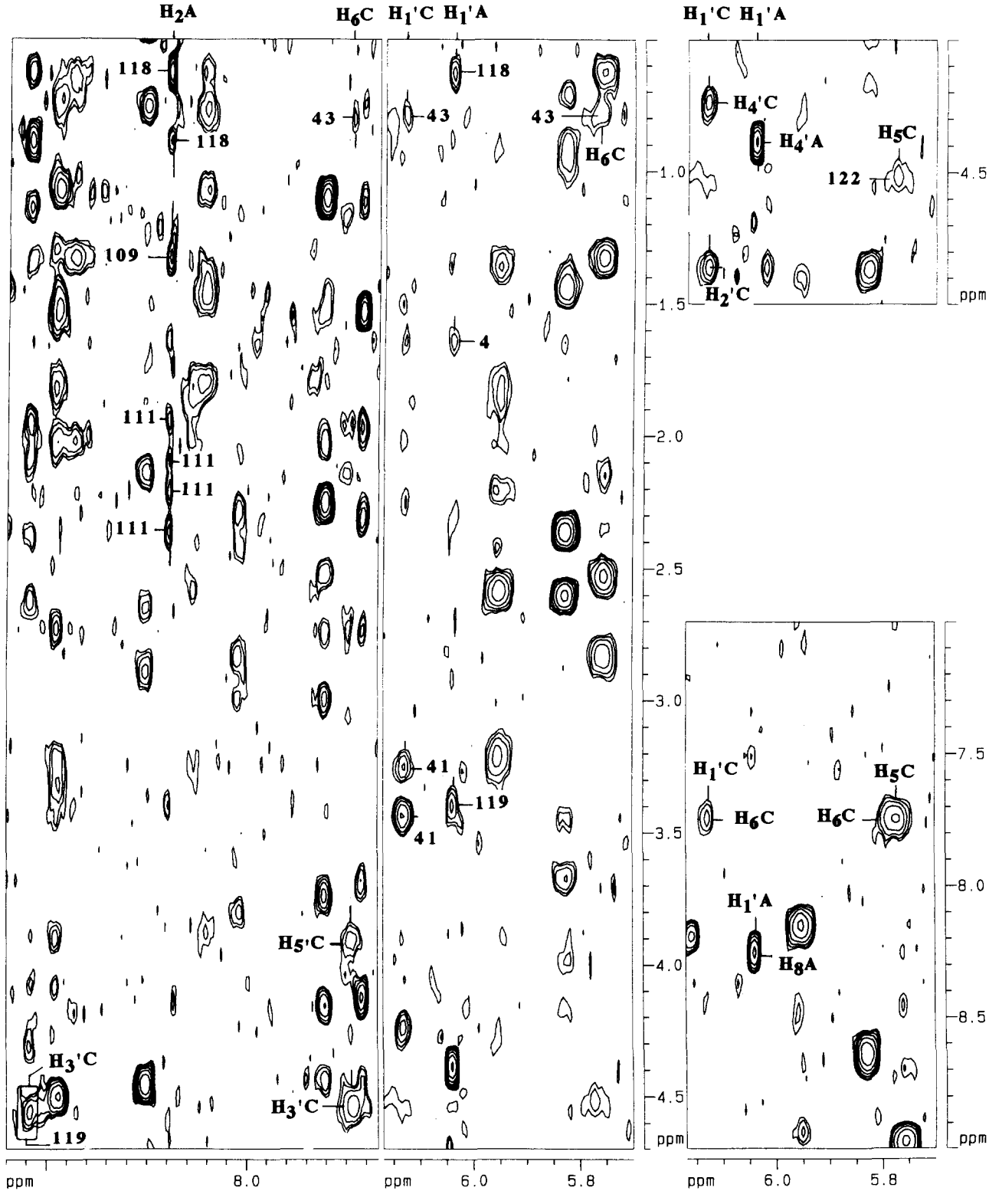

Fig. 2. Selected region of the two-dimensional NOESY spectra RNase A/2′,5′-CpA 1:1 complex (4 mM, pH 5.5, 35 °C, D_2O), showing intradinucleotide NOEs and intermolecular NOEs with Ala 4, Lys 41, Val 43, Ala 109, Glu 111, Val 118, His 119 and Ala 122.

ations on complex formation, indicating that the presence of the two nucleotide rings in the complexes is mainly responsible for the observed changes.

Resonances of the dinucleoside monophosphates also undergo chemical shift changes when bound to the enzyme (see Table 1). These variations are larger in the cytosine than in the adenosine

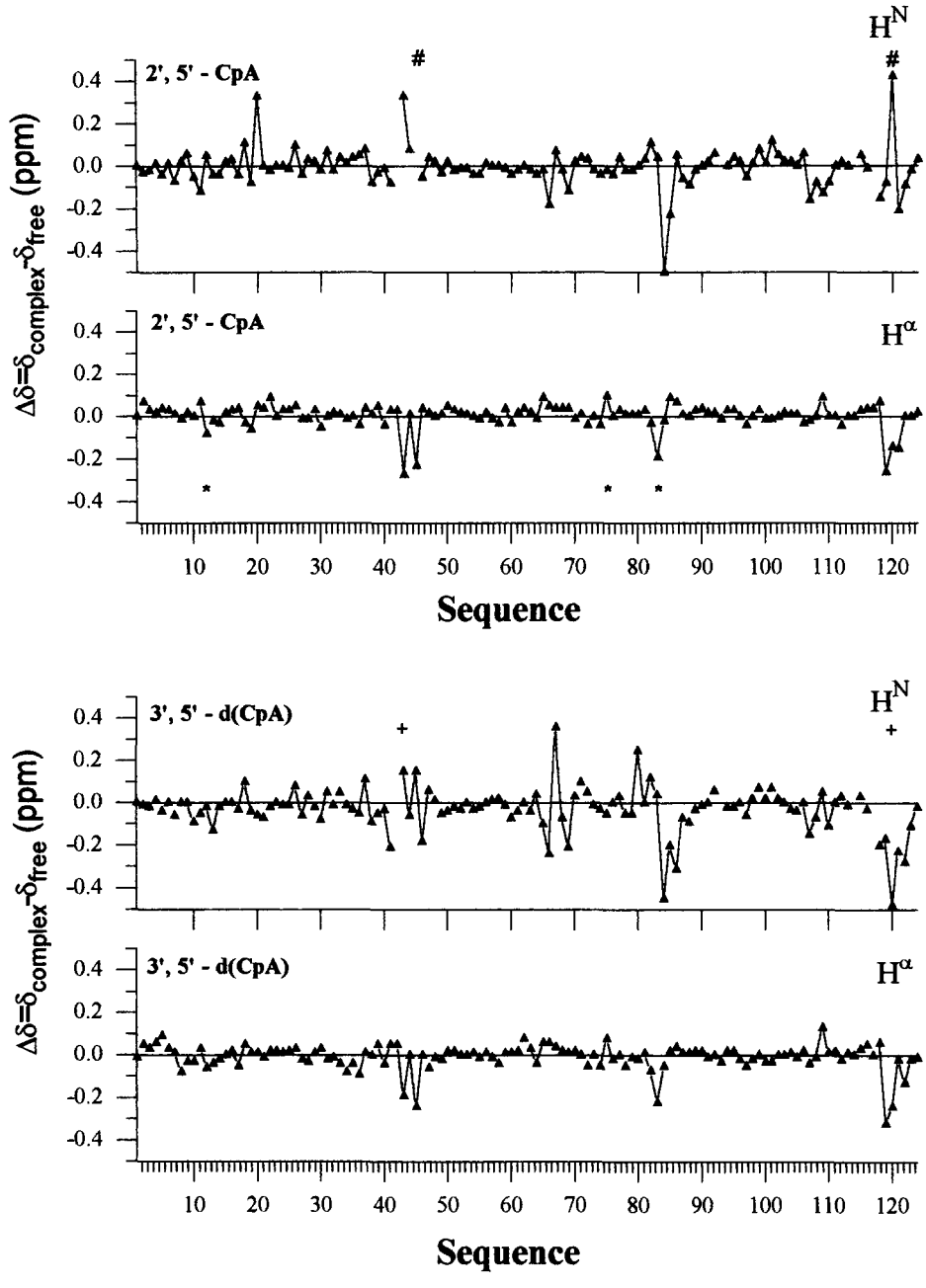

Fig. 3. Chemical shift variation on complex formation in the protein backbone resonances for RNase A/2′,5′-CpA (top) and RNase A/3′,5′-d(CpA) complex (bottom) for 1:2 complexes (pH 5.5, $T = 35$ degrees). *, only observed in the 1:1 complex; + and #, chemical shift measured at pH lower than 5.5.

moiety. In the 3′,5′-d(CpA) complex, the deoxycytidine protons H2′ and H2″ are particularly affected by the complexation, as shown by their chemical shift variation, which amounts to −0.66 and −0.47 ppm, respectively. In both complexes, changes in chemical shift of the adenine protons are very similar, with H8 being the one affected most (+0.19 ppm).

Distance constraints

Once it was accepted that no global changes in the structure of the protein occur with ligand binding, attention was focused on the differences between the complexes and the free forms of the enzyme rather than in a complete de novo structural determination. The analysis of the NOESY spectra was then confined mainly to signals from residues showing significant chemical shift changes. The pattern of intramolecular NOE constraints in both complexes is rather similar to that found in the free enzyme, though some differences in the NOEs corresponding to a few side-chain proton resonances were observed. Intramolecular constraints for either the enzyme or the ligand were derived from protein saturated or nucleotide saturated samples, respectively. Special attention was paid to detect intermolecular NOEs

Table 1. *Chemical shift variation on complex formation in the inhibitor resonances for the RNase A/2',5'-CpA and RNase A/3',5'-d(CpA) complexes*[a]

	2',5'-CpA		3',5'-d(CpA)	
	Cyt.	Ade.	Cyt.	Ade.
H8	–	−0.18	–	+0.19
H2	–	−0.12	–	+0.10
H6	+0.19	–	−0.25	–
H5	+0.24	–	−0.07	–
H1′	+0.13	−0.06	−0.19	+0.01
H2′	+0.16	+0.08	−0.66	+0.07
H2″	–	–	−0.47	+0.03
H3′	+0.16	0	−0.24	–
H4′	+0.15	−0.07	–	−0.11
H5′, H5″	–	–	–	−0.11

[a] ($\Delta\delta = \delta_{complex} - \delta_{free}$ ppm).

between the enzyme and each of the dinucleotides, which were derived from 1:1 samples. A total of 23 intermolecular contacts for the 3',5'-d(CpA) and 19 for the 2',5'-CpA complex could be detected. They are listed in Table 2. A number of these intermolecular NOEs as well as some intradinucleotide correlations are illustrated in Figure 1 [3',5'-d(CpA) complex] and in Figure 2 [2',5'-CpA)]. Except for the NOEs corresponding to the H2″ proton, which is lacking in 2',5'-CpA, most of the NOE cross-peaks involving the dinucleotide protons are common to both complexes. Thus, contacts are observed between the cytidyl moiety and protons in residues His 12, Lys 41, Val 43, His 119, and Ala 122 in both cases. In the complex with 3',5'-d(CpA), NOE cross-correlations were also detected for residues Phe 120 and Ser 123. On the other hand, NOE cross-correlations were observed in both complexes between the adenyl part of the ligands and residues Ala 4, Glu 111, Val 118, and His 119. An additional contact was observed with residue Ala 109 in the 2',5'-CpA complex.

Most of the intramolecular NOEs detected in the free enzyme are also found in the complexes. Especially interesting is the lack of conflicting NOEs in the side chain of His 119. In the free enzyme, the $H^{\delta 1}$ proton of His 119 showed strong NOE cross-peaks with protons of Asp 121 and with the two methyls of Val 118. No single position of the histidine ring could account for all the detected NOEs and two conformations of the side chain of His 119 were assumed to exist in a rapid conformational equilibrium, in order to satisfy all the constraints. In the two dinucleoside monophosphate complexes studied here, only the NOEs with Asp 121 were observed. A very weak NOE between one of the γ-methyl of Val 118 and $H^{\delta 1}$ of His 119 is observed in the two complexes, but the corresponding distance constraint (<6 Å) does not present any conflict.

Three-dimensional structures

As discussed in the chemical shift section, we have arrived reasonably to the conclusion that the structure of the protein in the complex must be very similar to that of free enzyme except in those regions where changes in the proton chemical shifts were detected. This chemical shift information has been implemented

Table 2. *Intermolecular distance constraints (Å) between pairs of protons as derived from a qualitative evaluation of NOE cross-correlations*

Proton pair				2',5'-CpA	3',5'-d(CpA)	3',5'-d(CpA) (RX)
$H^{\epsilon 1}$	12	H1′	Cyt	4.0	4.0	2.7
$H^{\epsilon 1}$	12	H2″	Cyt	–	5.0	2.5
P^{ϵ}	41	H1′	Cyt	–	ps 4.9[a]	6.7
$H^{\epsilon 1}$	41	H1′	Cyt	4.0	–	–
$H^{\epsilon 2}$	41	H1′	Cyt	3.0	–	–
$C^{\gamma 2}$	43	H6	Cyt	6.0	5.0	4.5
$C^{\gamma 2}$	43	H1′	Cyt	6.0	5.2	4.8
H^{β}	43	H1′	Cyt	–	4.5	4.4
H^{β}	43	H5	Cyt	–	4.5	4.9
$C^{\gamma 2}$	43	H5	Cyt	5.0	5.0	4.3
$H^{\epsilon 1}$	119	H3′	Cyt	5.0	–	2.6
$H^{\epsilon 1}$	119	P5′	Cyt	–	ps 5.9[a]	4.3
$H^{\epsilon 1}$	119	H2′	Cyt	–	5.0	3.6
$H^{\epsilon 1}$	119	H2″	Cyt	–	5.0	4.8
$H^{\epsilon 1}$	120	H5	Cyt	–	5.0	5.0
H^{α}	122	H5	Cyt	4.5	3.5	3.8
C^{β}	122	H5	Cyt	–	5.0	5.4
H^{N}	123	H5	Cyt	–	5.0	5.3
H^{α}	4	H1′	Ade	–	5.0	6.9
C^{β}	4	H2	Ade	–	6.0	6.6
C^{β}	4	H1′	Ade	6.0	–	6.2
C^{β}	109	H2	Ade	4.0	–	4.6
$H^{\beta 2}$	111	H2	Ade	5.0	–	–
$H^{\beta 3}$	111	H2	Ade	5.0	–	4.5
$H^{\gamma 1}$	111	H2	Ade	5.0	ps 4.9[a]	3.0
$H^{\gamma 2}$	111	H2	Ade	5.0	–	–
$C^{\gamma 2}$	118	H2	Ade	6.0	–	3.2
$C^{\gamma 1}$	118	H2	Ade	6.0	–	5.3
$C^{\gamma 2}$	118	H2	Ade	4.0	4.0	4.0
$C^{\gamma 2}$	118	H8	Ade	–	6.0	7.7
$H^{\beta 2}$	119	H1′	Ade	4.0	5.0	4.7
$H^{\epsilon 1}$	119	H8	Ade	5.0	5.0	3.8

[a] ps, distance constraint is set to the pseudo atom position. The corresponding correction in the distance limit is included.

in our molecular dynamics calculation by constraining the atomic position in all regions of the protein where there was no significant variation in chemical shifts. Residues with a binding chemical shift larger than a certain threshold have been allowed to move during the simulation (see Materials and methods). Thus, all residues involved in the active site and those which were found flexible in the free enzyme were not constrained. By adopting very conservative thresholds for the chemical shift variations (0.05 ppm for H^{α} and 0.1 ppm for H^{N} protons), a total of 72 residues were constrained in their backbone and 62 more in their side chains. Constrained and nonconstrained residues are displayed in different colors in Kinemage 6 in the Electronic Appendix.

Residual distance constraint violations as well as values of the most significant energy terms in the final structures are given in Table 3. No distance restraint is violated by more than 0.9 Å in any of the resulting structures. The final structures fulfil all the intermolecular restraints with very small residual violations. Only minor average deviations from ideal geometry (bond lengths, bond angles, and improper torsion angles) are observed.

Table 3. *Structure statistics*[a]

Range	Complex	
	2′,5′-CpA	3′,5′-d(CpA)
0.10–0.25	27.9	44.0
0.25–0.50	20.1	18.6
0.50–0.75	1.6	5.7
0.75–1.00	1.7	0.4
>1	0	0
Max. viol. (Å)	0.9	0.7
Sum of viol. (Å)	12.0	16.6
Ave. total energy[b]	−8,573	−8,428
Total energy range	−8,934 to −7,976	−9,411 to −8,025
Ave. Lennard-Jones energy	−4,730	−4,657
Lennard-Jones energy range	−4,774 to −4,678	−4,715 to −4,560
Ave. NOE term	117	151
NOE term range	104–130	107–137

[a] Average values for the eight resulting structures of each complex.
[b] Energy units are kJ/mol.

The structures show large and negative values of the Lennard-Jones and electrostatic energy terms, comparable to the ones obtained for the free enzyme (Santoro et al., 1993). In spite of the additional restraint concerning the atomic position of a large number of residues introduced in the calculation, the residual distance constraint violation in the final structures was very small. This indicates that the experimental distance constraints obtained from the NOE data are consistent with the restraints imposed on the basis of the chemical shift information.

Overall, the resulting structures are well-defined, with a pairwise RMS deviation (RMSD) of 0.2 Å [3′,5′-d(CpA)] and 0.3 Å (2′,5′-CpA) for the protein backbone and 1.4 Å (both complexes) if the side chains are included. Figure 4 shows the RMSD of the backbone torsion angles for the two complexes. The largest deviation (region 87–88) corresponds to one of the most flexible regions of the free enzyme. Differences in this loop region are not related to the presence or absence of an inhibitor, because analogous profiles are observed when representing the RMSDs of independently converged structures of the free enzyme as a function of the sequence. The C-terminal region also shows a significant deviation in the 3′,5′-d(CpA) complex, which

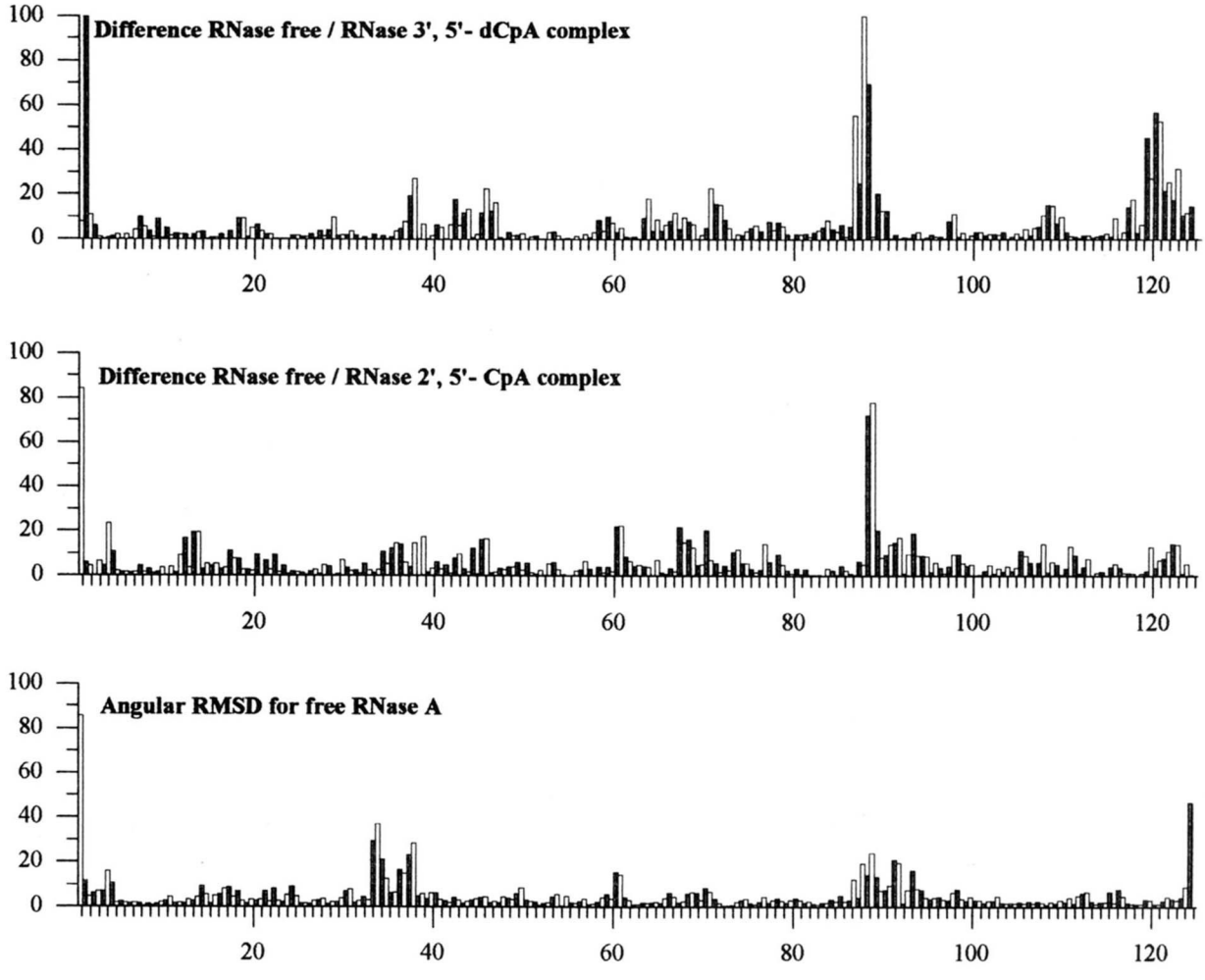

Fig. 4. Differences in the backbone torsion angles (ϕ in white and ψ in black) between the free enzyme and the two RNase A/dinucleotide complexes, compared with RMSD for the same angles in the free enzyme.

is concentrated in residues 119–122. Figure 5 shows a superposition of the active site in the eight final structures for both complexes. The average structures are displayed in Figure 6. The relatively large RMSD of the inhibitor atoms (1.2 Å) do not have their origin in the base and sugar moieties of both dinucleotides, which are well defined, but in the connecting regions between the two sugars (the phosphodiester group). This poor definition is due to the lack of NOE-derived experimental constraints in this part of the molecule. Some of the protein side chains that are involved in the ligand binding, or are very close to it, are well-defined, such as His 12, Thr 45, Val 43, His 119, and Phe 120. Other residues, like Gln 11 and Lys 66, in the proximity of the phosphate binding site, or Asn 67, Gln 69, and Asn 71, involved in the adenine binding site, present a more flexible structure. The intermolecular hydrogen bonds observed in most of the final structures are listed in Table 4.

The structure of the active site is very similar in the two complexes (see Kinemages 1, 2, and 3). His 12 maintains the same position as in the free enzyme, forming a hydrogen bond involving the imidazolic $H^{\delta 1}$ and the carbonyl oxygen of Thr 45. The proton $H^{\epsilon 2}$ on the other side of the imidazole ring is hydrogen bonded to one of the phosphate oxygens. In general, the hydrogen bond is not formed with the same phosphate oxygen in all converged structures, but the difference affects only to the relative position of the oxygen around the phosphorous atom. Thr 45 participates in the binding process, forming two hydrogen bonds: one involving the backbone H^N atom and the carbonyl oxygen of the cytidine base, and another involving the hydroxylic proton of the side chain and the nitrogen atom in position 3 of the same base. On the opposite side of the active center, the backbone H^N proton of Phe 120 is hydrogen bonded to one of the oxygens of the phosphodiester group as well as the imidazolic $H^{\delta 1}$ proton of His 119, which interacts preferentially with the ester oxygen O5′. The adenine base is involved in several transient hydrogen bonds with Asn 67, Gln 69, and Asn 71. None of these bonds has a population larger than 25% in the final set of calculated structures, and this is why they are not included in Table 4. The position of the adenine base is almost identical in all the structures. Differences arise from the different conformation adopted by the side chain of residues 67, 69, and 71, which are shown as highly flexible in the solution structures.

Although NOE cross-correlations between the H^{ϵ} protons of Lys 41 and H1′ of the cytidyl ribose ring have been detected in

Table 4. *Close contacts (X···A distances lower than 3.5 Å) between atoms of RNase A and the ligand*

		2′,5′-CpA	Distance X···A (Å)	3′,5′-d(CpA)	Distance X···A (Å)
Gln 11	$H^{\epsilon 2}$	–	–	Cyt O3′	3.2
His 12	$H^{\epsilon 2}$	O1P-O2P[a]	3.0	O2P[a]	3.0
Thr 45	$O^{\gamma 1}$	H42	2.9	H42	3.0
Thr 45	$H^{\gamma 1}$	–	–	Cyt N3	3.1
Thr 45	H^N	O2	3.5	O2	3.1
His 119	$H^{\delta 1}$	Ade O5′-O4′	3.0	Ade O5′-O4′	3.2
Phe 120	H^N	O2P[a]	2.9	O2P[a]	3.4
Asp 121	O	H41	3.1	–	–

[a] O1P and O2P refer to oxygen bound to the phosphorous atom.

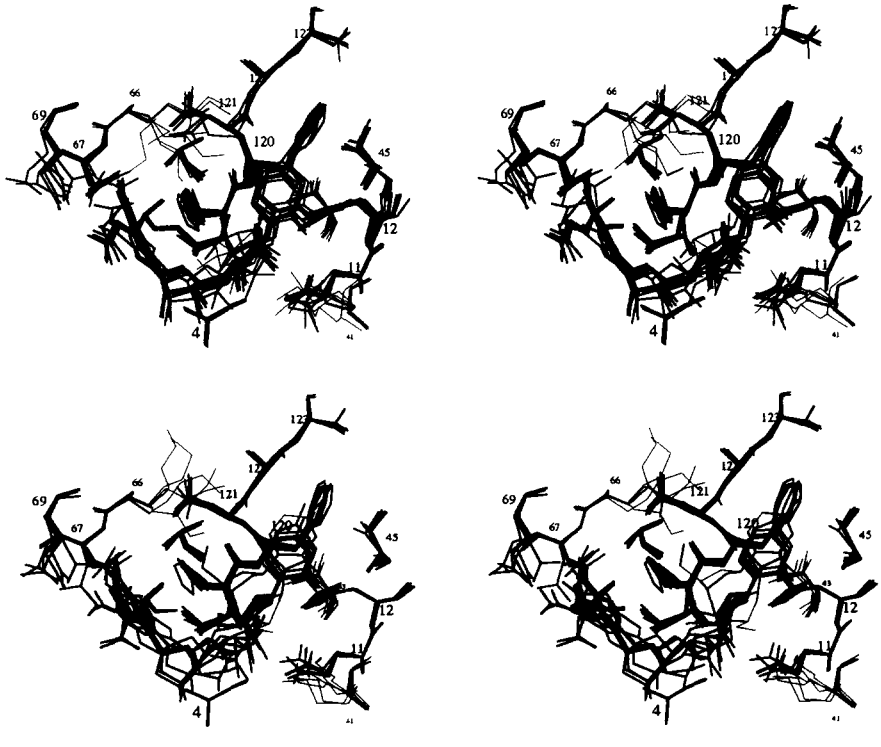

Fig. 5. Stereo view of the active site of RNase A/dinucleotide complexes. Top: superposition of the eight final structures of RNase A/3′,5′-d(CpA) complex. Bottom: superposition of the eight final structures of RNase A/2′,5′-CpA complex.

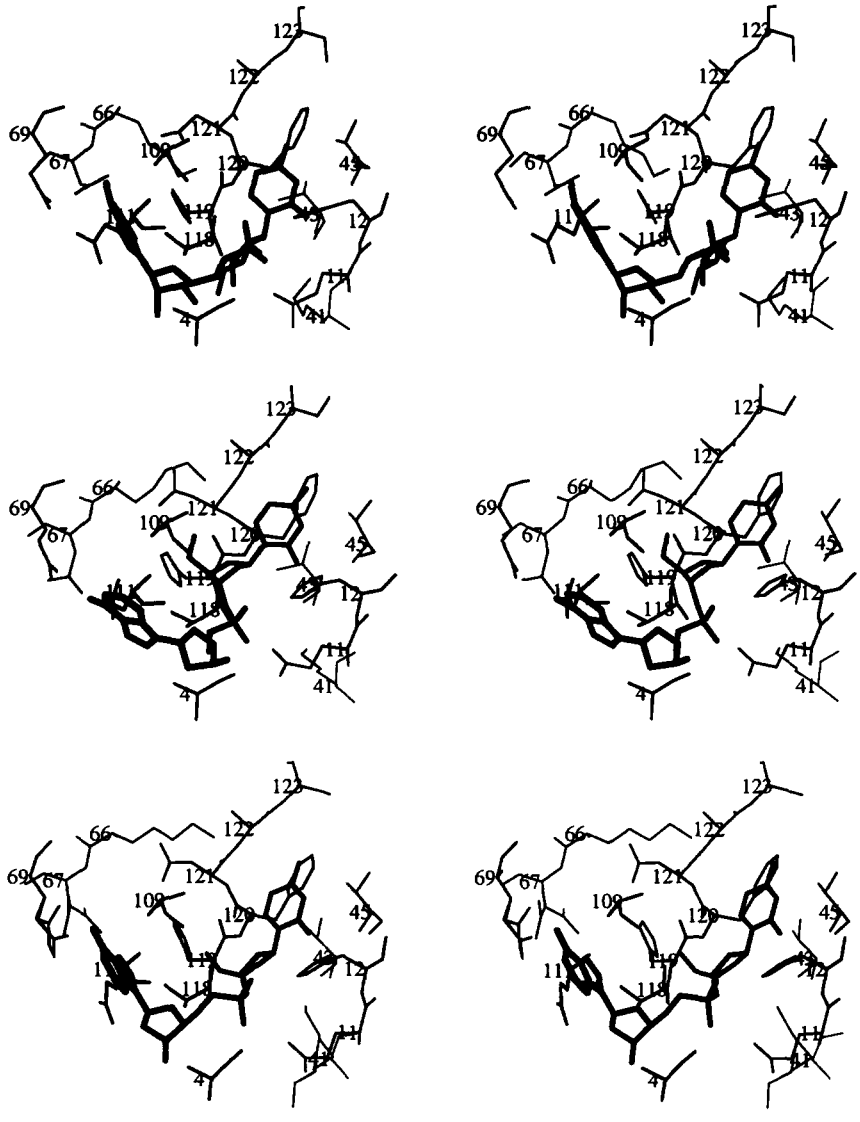

Fig. 6. Stereo view of the active site in the average solution structures compared with the crystallographic one. Top: RNase A/2′,5′-CpA complex. Middle: RNase A/3′,5′-d(CpA) complex (solution structure). Bottom: RNase A/3′,5′-d(CpA) complex (X-ray structure).

both complexes, no hydrogen bond appears in the final structures attributable to the ammonium group of this residue. This may be due to the lack of enough constraints to define completely the conformation of this side chain, which, in any case, is located closer to the phosphate than in the initial structure. The H^{ϵ} protons of Gln 11 form hydrogen bonds with the cytidyl sugar O3′ atom in the 3′,5′-d(CpA) complex, although no NOE cross-peak is observed between Gln 11 and the inhibitor protons. This interaction is not observed in the 2′,5′-CpA complex. Lys 66 and Ser 123 have been also considered as part of the active site of RNase A, but no direct hydrogen bond interaction is observed in the solution structures. In the crystallographic structures available, these interactions are often mediated by a water molecule. As discussed previously, the chemical shifts of the side-chain protons of Gln 11, Lys 66, and Ser 123 change on complex formation, what may be an indication of their playing a role, albeit indirect, in the binding process. Chemical shift of the methyl protons of Val 43 are largely affected by complex formation. They also show several NOE cross-peaks with the inhibitor protons. In agreement with these experimental data, in the calculated structures this residue is in close contact with the ribose ring of the cytidine. Whereas the $\chi 1$ angle of the side chain of Val 43 is not well-defined in the free enzyme due to motional averaging, the conformation of this side chain becomes remarkably less flexible in the complexes, up to the point that, in the RNase A/2′,5′-CpA complex, all resulting structures present values of $\chi 1$ angle in the g^- conformation.

As mentioned in the previous section, no conflicting NOEs were observed for the side chain of His 119 in the dinucleotide complexes, where only the NOEs with Asp 121 are observed. As a consequence, the resulting structures from restrained molecular dynamic calculations correspond exclusively to conformation A in the free enzyme. A visual inspection of the solution structures of the dinucleotide complexes indicates that the sec-

ond position of the His 119 in the free enzyme is now occupied by the adenine base (Fig. 7).

Some structural features of the two inhibitor molecules in the final structures are shown in Table 5. Glycosidic torsion angles in the 2′,5′-CpA complex are in the anti conformation in both dinucleotides ($\chi = -123$ degrees for the cytosine and -77 degrees for the adenosine moiety). The sugar conformations are in the general N-domain, with pseudorotation phase angles of 80 degrees (cytosine) and 42 degrees (adenine) corresponding to the C4′-exo region. Both bases are also in the anti conformation in the 3′,5′-d(CpA) complex, with values for the glycosidic angle of -145 degrees and -107 degrees for the cytosine and adenosine moieties, respectively. However, sugar ring conformations are in the two nucleosides in the general S-domain with pseudorotation angles of 124 degrees (C1′-exo) and 181 degrees (C2′-endo), respectively. Some distortion is observed in the geometry of the cytidine sugar ring, arising probably from internal inconsistencies in the set of NOEs. Remarkably, the sugar conformations obtained for the 3′,5′-d(CpA) complex by X-ray crystallography are in a N-type domain. To further check this discrepancy between the crystal and solution structures, the ^{3}J coupling constants between the sugar protons in the two complexes were analyzed.

Values for coupling constants of the ribose rings were obtained from the phase-sensitive DQF-COSY spectra by computer simulations of the COSY cross-peaks. In these simulations, the experimental conditions, such as line widths or apodization functions, are reproduced by the program, and the ^{3}J coupling constants involved are varied manually until a good match with the experimental cross-peak is achieved. Figure 8 shows an example for the adenine sugar protons in the 3′-5′d(CpA) complex. Coupling values are related to dihedral angles of the ribose ring through a modified Karplus equation (Wijmenga et al., 1993). In this case, the values obtained confirm that sugar puckers are in the general S-domain in the two cases. Especially informative to discard N-type sugar conformations is the H1′-H2′ coupling constant, which must be very small for rings with low pseudorotation phase angles (N-type). In the case of the 3′-5′d(CpA) complex, the H1′-H2′ ^{3}J coupling constant is 8.0 Hz and the H1′-H2″ is 6.0 Hz for the adenosine (Fig. 8). The ^{3}J coupling constants for the cytosine are in the same range, but they could not be estimated accurately because of the broader line widths in the sugar protons of this nucleotide. In both cases, the values are only consistent with sugar puckers in the general S-domain.

In the case of 2′-5′CpA complex, $^3J_{1'2'}$ coupling constants are very small in both nucleotides, as can be seen from the lack of H1′H2′ cross-peak in the COSY spectrum. This indicates that sugar conformations are in the N-domain (low pseudorotation phase angles), a result that agrees with the pseudorotation phase angles obtained in the calculated structures, as can be seen in Table 5. Because the H1′-H2′ coupling constant in the free dinucleotide are both approximately 5 Hz, the N-type conformation of the riboses is induced by the binding of RNase A.

Comparison of the solution structure of the complex with the crystal structure

A comparison of the solution structure of the RNase A/2′,5′-CpA complex with that determined in the crystal state for the complex RNase A/2′,5′-CpA (Wodak et al., 1977) cannot be made in detail because the Cartesian coordinates of the latter are lacking. However, we can compare the data relative to the structure of the ligand as well as the close contacts and relevant interactions found between atoms of the protein and of the inhibitor. The torsional angles are compared in Table 5. Also, a superposition of the structure of the complexed 2′,5′-CpA in solution and in the crystal state is given in Kinemage 5 included in the Electronic Appendix. Although there are large differences in some torsion angles, particularly in the γ (Ade) and α, the global shape of the bound ligand and the topological location of the two bases, the two sugar rings, and the phosphate groups coincide. This is because the two structures differ mainly in a concerted change the two above torsion.

In relation to the enzyme–inhibitor hydrogen bonds, those observed in solution are also observed in the crystal, with the exception of the one between the carbonyl oxygen in position 2 of the cytidine base and the amide proton of the Thr 45. It is of note that in the early crystallographic work of Wodak et al. (1977), model building and energy minimization were used in conjunction with difference Fourier techniques, and, as recognized by the authors, relatively noisy maps precluded an unambiguous and detailed interpretation. We think that our solution structures based on experimental data (NOE cross-correlations and coupling constants) have a higher level of reliability and accuracy.

The glycosidic as well as the backbone torsion angles of the solution and crystal structures of the complex RNase A/3′,5′-d(CpA) are very similar indeed (see Table 5), with the only exception of the unimportant exocyclic torsion γ (Cyt). The active site in these

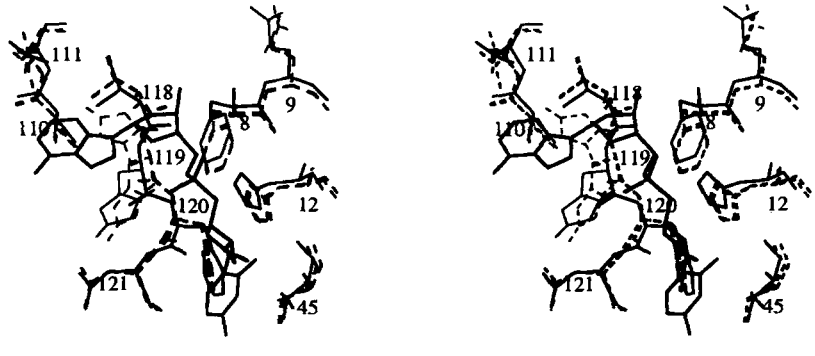

Fig. 7. Stereo view of the active site of RNase A. Superposition of the free enzyme structure with the two positions of the side chain of His 119 (dotted lines) and the RNase A/3′,5′-d(CpA) complex (solid lines).

Table 5. *Averaged structural parameters of the dinucleotides in the RNase A/inhibitor complexes*

	2′,5′-CpA				2′,5′-CpA X-Ray (Wodak et al., 1977)		3′,5′-d(CpA)				3′,5′-d(CpA) X-Ray (Zegers et al., 1994)	
	Cyt	Range	Ade	Range	Cyt	Ade	Cyt	Range	Ade	Range	Cyt	Ade
Glycosyl torsion angle (deg)												
O1′-C1′-N9-C4 (χ)	−123	−132···−115	−77	−91···−72	−107	−82	−145	−160···−128	−107	−121···−95	−155	−103
Sugar torsion angles (deg)												
C4′-O1′-C1′-C2′ (ν0)	−39	−47···−25	−19	−14···27	4	7	−39	−45···−29	−23	−37···−10	−18	−24
O1′-C1′-C2′-C3′ (ν1)	19	4···29	−11	−18···−3	−25	−28	36	25···41	38	28···46	25	37
C1′-C2′-C3′-C4′ (ν2)	7	0···22	35	30···40	36	37	−18	−39···−7	−38	−42···−34	−22	−35
C2′-C3′-C4′-O1′ (ν3)	−32	−34···−27	−48	−50···−46	−38	−36	−5	−17···23	26	19···34	11	22
C3′-C4′-O1′-C1′ (ν4)	43	37···46	42	40···46	22	19	27	4···39	−2	−12···11	5	1
Phase	80	61···90	42	36···52	16	10	124		181		−28.6	−20.4
Backbone torsion angles (deg)												
O5′-C5′-C4′-C3′ (γ)	−122[a]	−177···171	52	47···61	−83	154	128[a]	−178···179	179[a]	−179···172	31	172
C5′-C4′-C3′-O3′ (δ)	84	72···89	64	58···73	105	87	114	105···142	145	139···154	122	139
Phosphodiester torsion angles[b]												
O3′(O2′)-P-O5′-C5′ (α)			124[a]	−141···150		−31			90[a]	−168···116		77
P-O5′-C5′-C4′ (β)			164[a]	−179···180		172			146[a]	−113···160		110
C4′(C3′)-C3′(C2′)-O3′(O2′)- P (ε)	−96[a]	−170···78			−131		−144	−175···−79			−160	
C3′(C2′)-O3′(O2′)-P-O5′ (ζ)	54	−159···133			120		64[a]	−114···88			55	

[a] Average value for the most populated conformer.
[b] Atoms in brackets correspond to 2′,5′-CpA.

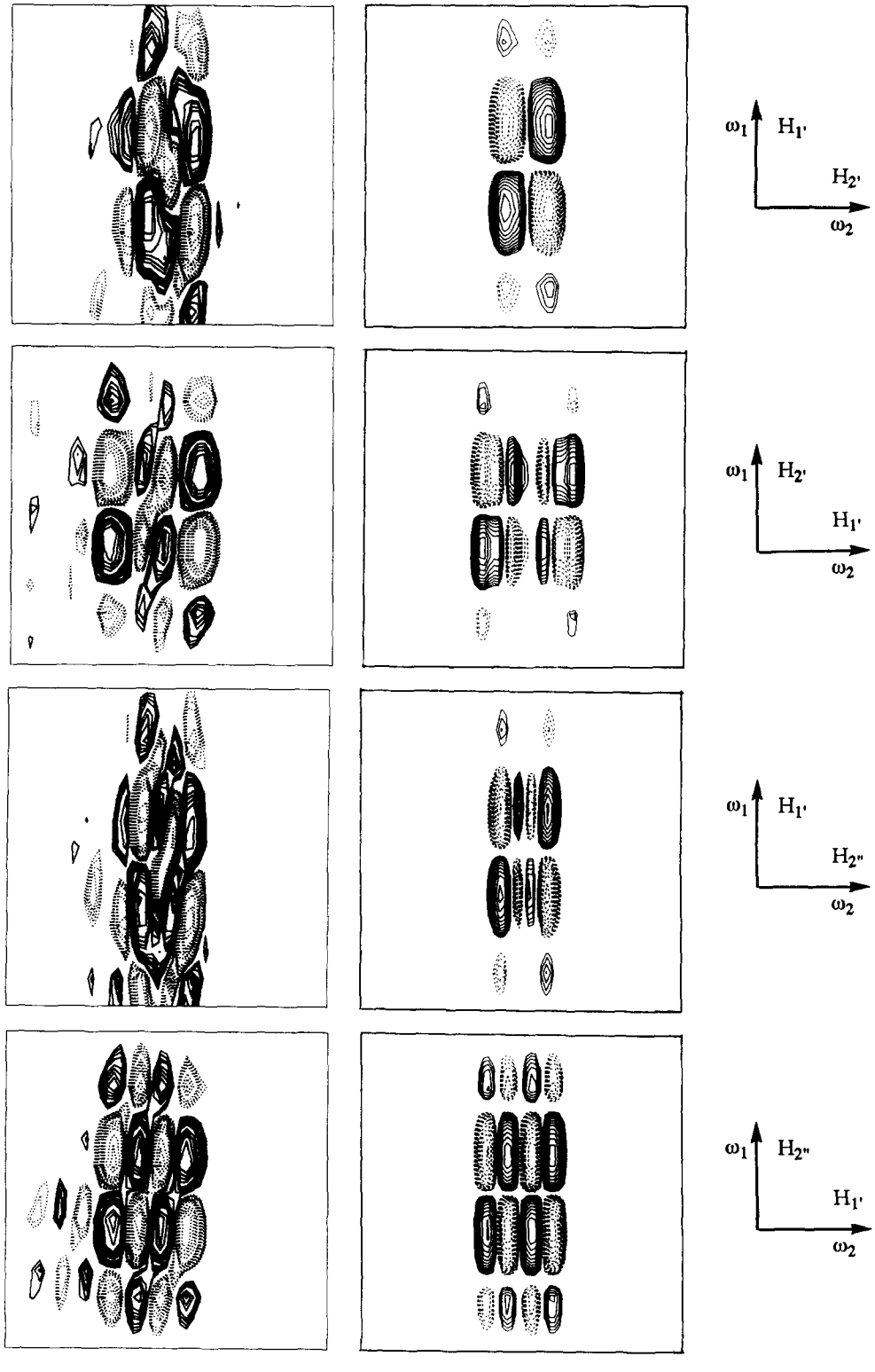

Fig. 8. Simulation of the DQF-COSY cross-peaks of the adenosine deoxyribose proton spin system of the 3',5'-d(CpA)-RNase 1:1.5 complex. Left side, experimental cross-peaks. Right side, simulated cross-peaks.

two structures are compared in Figure 6. This figure has been included as Kinemages 1 and 4 in the Electronic Appendix for a more detailed and complete comparison. Also, most of the observed intermolecular interactions between the inhibitor and the protein are common to both structures (see Table 4, and Table 3 of Zegers et al., 1994). Although the position of the dinucleotide in the solution and crystallographic structures is very similar, there are important differences in the conformation of the

dinucleotide (see Table 5). The main difference affects the sugar conformation of the deoxyriboses. Whereas the pseudorotation phase angles in the crystallographic structures are small (in the general N-domain), the solution structures present large values (characteristic of the general S-domain). As mentioned previously, these sugar conformations, resulting from the restrained molecular dynamics calculation, were confirmed by direct experimental evidence arising from the J coupling values between the deoxyribose protons. These results suggest that crystal packing may affect the conformation of the deoxyriboses in the RNase A/3′,5′-d(CpA) complex. Similar conclusions have been obtained in other related complexes, such as the 3′-GMP/barnase complex (Meiering et al., 1993) and several mononucleotide/RNase T1 complexes (Inagaki et al., 1985).

Discussion

The solution structures of the complexes of RNase A with 2′,5′-CpA and 3′,5′-d(CpA) determined herewith very closely resemble those of the structures determined previously for the two complexes in the crystal state. As in that case, it is remarkable the lack of any large conformational change in the enzyme to accommodate the inhibitors, a fact that is strongly supported by the chemical shift variation on complex formation as well as by an almost identical pattern of observed NOEs in the free and bound forms of the enzyme.

The mode of binding obtained for these complexes is the standard or productive one, which may provide insights into the binding and catalysis of actual substrates. This is in contrast to the results found for the complexes of RNase A with 2′,5′-CpG and 3′,5′-d(CpG) (Aguilar et al., 1991, 1992; Lisgarten et al., 1995), according to which the inhibitors are bound in a nonproductive way (retro-binding in the words of the authors) in which the downstream guanine is bound at the major binding site. As concluded by Zegers et al. (1994), retro-binding must occur between guanine and the residues at the major binding site.

In spite of their structural differences, the two dinucleoside monophosphates are recognized by the enzyme in much the same way. Recognition is accomplished through the same set of inhibitor–enzyme-specific interactions, which, as detailed previously, involves Thr 45 in the binding of the cytidine base and His 12, His 119, and Phe 120 as the interacting residues with the oxygen atoms of the phosphodiester group. The Lys 41 extended side chain moves closer to the phosphate group with respect to the free enzyme, which is in agreement with the role assigned to this residue of stabilizing electrostatically the transition state.

On the basis of crystallographic and NMR studies of RNase-nucleotide complexes, together with an affinity labeling approach, de Llorens et al. (1989) have built a tentative model of a complex of RNase A with a pentadeoxynucleotide in which a rather extensive binding region comprising multiple specific subsites was proposed. Some of the predictions generated by their study were tested by a crystal structure determination of a related pentadeoxynucleotide (Fontecilla-Camps et al., 1994). Subsite B2, corresponding to the downstream adenine in our complexes, is clearly delineated in that work as an specific binding site, in agreement with the results obtained for the crystal structure of the complexes of RNase A with 3′,5′-d(CpA) (Zegers et al., 1994) and 2′,5′-CpA (Wodjak et al., 1977). Interactions in that site may contribute to the complex stability as well as to properly orientate the scissible P-O5′ (Ade) bond. The location of the adenine base in the solution structure of these two complexes is also remarkably well-defined and its position coincides practically with that determined in the crystal structures. The side chains of Gln 69, Asn 71, and Glu 111 were found to interact by hydrogen bonding with the adenine base in the crystal state of the 2′,5′-CpA complex (Wodjak et al., 1974), whereas in the 3′,5′-d(CpA) complex, Zegers et al. (1994) found that only the side chain of Asn 71 formed two parallel strong bonds with the adenine base. This is in agreement with the results of Tarragona-Fiol et al. (1993), who mutated the residues Gln 69, Asn 71, and Glu 111 and found that only the Asn 71 Ala mutation lowers the transesterification rate significantly. However, Fontecilla-Camps et al. (1994), in their study on the crystal structure of the complex of RNase A with d(ApTpApApG), found that the side chains of both Gln 69 and Asn 71 interact with the downstream adenine base. This is more in agreement with the results obtained for the solution structures, for which we have found transient hydrogen bonds of the side chains of Gln 69 and Asn 71 and even of Asn 67 with the adenine base. It may be, as stated by Fontecilla-Camps et al. (1994), that the side chains of all those residues constitute a malleable binding site capable of establishing a variety of hydrogen bonds depending on the nature of the base to be bound.

Some comments on the structure of the bound inhibitors seem pertinent. The conformation of the base around the glycosidic bond is in the anti region in all cases, in agreement with the structure of the complexes in the crystal state. However, the sugar conformation of the cytidine and adenine nucleotides in the complex with 3′,5′-d(CpA) is in the S region in the solution structure at variance with that found for this complex in the crystal state (Zegers et al., 1994). The coupling constant information appears to be extremely valuable in defining the sugar conformation, which may have an influence on the conformation of the ribose-phosphate backbone of the substrate. On the other hand, the NMR method, when based exclusively on NOE effects, is of limited use in defining the phosphate backbone. An integrated approach of the two techniques, NMR and X-ray diffraction, may help in obtaining the structure of the ligand in considerable detail.

Finally, the solution structure of the two complexes reveals another important point that was observed previously in the crystal structure and that is related to the two positions found for the His 119 side chain in the free enzyme. The presence of the downstream adenine base blocks the alternative position (position B) that this side chain is able to adopt in the free enzyme. Thus, in the two complexes, we are only left with position A, in which the imidazolic group is hydrogen bonded to O5′ in the phosphodiester group (through $NH^{\delta 2}$) and to one $O\epsilon$ in the carboxylate group of Asp 121 (through $NH^{\epsilon 1}$). According to these facts, and in agreement with that stated by Zegers et al. (1994), it seems more probable that His 119 is active in the A conformation during the transesterification reaction.

Materials and methods

Sample preparation

RNase A was purchased from Worthington and used without further purification. The protein was dissolved in either H_2O/D_2O (9:1) or D_2O (1:1). Complexes were obtained by adding 25 mg of RNase A and the corresponding amount of dinucleo-

tide (1.08 mg for 3′,5′-d(CpA) or 1.14 mg of 2′,5′-CpA), resulting in a sample of 4 mM concentration. Samples with different stoichiometry were also prepared to achieve either complete protein saturation (1:2) or complete inhibitor saturation (2:1). Due to serious overlapping, spectra were recorded over a range of temperature (5–40 °C). Because the pH for optimal binding was 5.5, spectra were recorded in a range of pH from 4.0 to 5.5 as an aid for a more direct translation of the free enzyme assignments obtained at pH 4.0 (Rico et al., 1989) to the complexes.

NMR experiments

NMR spectra were recorded in a Bruker AMX spectrometer operating at 600 MHz. 2D spectra were acquired in the phase-sensitive mode using the time-proportional phase incrementation technique (Marion & Wüthrich, 1983). COSY, TOCSY, and NOESY were performed by acquiring 2,048 data points in $t2$ and 512 data points in $t1$. The spectra were zero-filled and Fourier transformed, giving a data matrix of 4,096 ($f2$) and 1,024 ($f1$). NOESY experiments were recorded with mixing times of 50, 100, and 200 ms. Coupling constants were extracted from DQF-COSY experiments (Rance et al., 1983). These spectra were recorded with 4,096 data points in $t2$ and 512 data points in $t1$. After zero-filling, a frequency domain data set of 4,000 × 1,000 was obtained with a digital resolution of 1.97 Hz/point in $f2$ and 5.88 Hz/point in $f1$. In both dimensions, a sine-squared apodization function shifted by $\pi/8$ was used for resolution enhancement. All spectra were processed with the Bruker software package UXNMR.

DQF-COSY simulations

SHINX and LINSHA programs (Widmer & Wüthrich, 1986) were used to simulate DQF-COSY cross-peaks for the ribose spin systems involving H1′, H2′, H2″, H3′, and H4′. SPHINX was used to calculate stick-spectra. All protons except H2′ and H2″ were treated as weakly coupled nuclei. The experimental conditions (digital resolution, apodization functions, truncation of the FID) as well as the natural line widths were incorporated into the simulated spectra with the program LINSHA. J coupling constants and line width were varied until an optimal matching between experimental and simulated cross-peaks was achieved.

Distance constraints

Interproton distance constraints were obtained from the analysis of NOESY spectra. To avoid contamination from the free species in the quantification of the NOE cross-peaks, intramolecular constraints were derived from either protein-saturated (RNase/inhibitor 1:2) or nucleotide saturated (RNase/inhibitor 2:1) samples. Intermolecular NOEs between the enzyme and the dinucleotides were derived from 1:1 samples. NOESY cross-peaks were integrated with the software package AURELIA (Neidig et al., 1995). Distance constraints were obtained from the cross-peak volumes by using the isolated spin-pair approximation. To avoid spin-diffusion effects, the distance constraints were evaluated from NOESY experiments recorded at shorter mixing times (50 ms).

Structure calculation

In order to obtain a starting structure for the molecular dynamics refinement, a preliminary docking of the different inhibitors with the average structure of the free enzyme was conducted. The docking was performed manually with the computer modeling package Insight II (Biosym Technologies Inc., San Diego, California). The inhibitor was placed in the interior of the active site in a conformation that roughly satisfied the experimental intermolecular distance constraints.

A total of eight structures was calculated for each complex. The calculation of these structures was performed by using restrained molecular dynamics methods as implemented in the package GROMOS (van Gunsteren & Berendsen, 1987), and following an annealing strategy similar to the one used in the structural calculation of the free enzyme (Rico et al., 1991, 1993). The structures were first energy-minimized, and then heated to 1,000 K. At this temperature, 40 ps of restrained molecular dynamics were conducted and eight structures were extracted from the trajectory, one every 5 ps. These structures were submitted to a cooling procedure of 5 ps, and an additional equilibration period at 300 K. This last part of the trajectory was used for averaging, and was followed by a final energy-minimization. The force constant for the experimental NOE term was 40.0 $kJ \cdot mol^{-1} \cdot Å^{-2}$ during the complete run.

Because chemical shift changes on complex formation are found in very well-defined regions of the protein, only the residues with a chemical shift change larger than a certain threshold were allowed to move during the simulation. Thus, the backbone atoms of residues with H^N shift deviation lower than 0.10 ppm or H^α chemical shift variation lower than 0.05 ppm were kept fixed. A similar criterion was used for the side chains. Atoms that were not moved during the calculation were kept fixed by adding an extra term to the standard GROMOS force field, which consisted of a quadratic penalty function with a force constant of 90.0 $kJ \cdot mol^{-1} \cdot Å^{-2}$. Other details of the calculation are identical to the free enzyme study (Santoro et al., 1993).

Acknowledgments

We thank Mr. Apolo Gómez, Mrs. Cristina López, and Mr. Luis de la Vega for excellent technical assistance. This work was supported by the Spanish Dirección General de Investigación Científica y Técnica, project n. PB93-0189.

References

Aguilar CF, Thomas PJ, Mills A, Moss DS, Palmer RA. 1992. Newly observed binding mode in pancreatic ribonuclease. *J Mol Biol 224*:2665–2676.

Aguilar CF, Thomas PJ, Moss DS, Mills A, Palmer RA. 1991. Novel non-productively bound ribonuclease inhibitor complexes-high resolution X-ray refinement studies on the binding of RNase A to (2′,5′-CpG) and 3′,5′-d(CpG). *Biochim Biophys Acta 1118*:6–20.

Blackburn P, Moore S. 1982. Pancreatic ribonuclease. In: Boyer PD, ed. *The enzymes XV*. New York: Academic Press. pp 317–433.

Borkakoti N, Moss DA, Palmer RA. 1982. Ribonuclease A: Least squares refinement of structure at 1.45 Å resolution. *Acta Crystallogr B 38*:2210–2217.

Borkakoti N, Palmer RA, Haneef I, Moss DS. 1983. Specificity of pancreatic ribonuclease A. An X-ray study of a protein–nucleotide complex. *J Mol Biol 169*:743–755.

Bruix M, Rico M, González C, Neira JL, Santoro J, Rüterjans H. 1991. Two-dimensional ^{1}H-NMR studies of the solution structure of RNase A-pyrimidine-nucleotide complexes. In: de Llorens R, Cuchillo C, eds.

Structure, mechanism and function of ribonucleases. Barcelona: Universidad Autùnoma. pp 15-20.

Crestfield AM, Stein WH, Moore S. 1963. Alkylation and identification of the histidine residues at the active site of ribonuclease. *J Biol Chem 238*: 2413-2420.

de Llorens R, Arús C, Parés X, Cuchillo CM. 1989. Chemical and computer graphic studies on the topography of the ribonuclease A active site cleft. A model of the enzyme-pentanucleotide substrate complex. *Protein Eng 2*:417-429.

Eftink MR, Biltonen RL. 1987. Pancreatic ribonuclease: The most studied endoribonuclease. In: Neuberger A, Brocklehurst K, eds. *Hydrolytic enzymes*. Amsterdam: Elsevier. pp 333-376.

Findlay D, Herries DG, Mathias AP, Rabin BR, Ross CA. 1962. The active site and the mechanism of action of bovine pancreatic ribonuclease 7. The catalytic mechanism. *Biochem J 85*:152-153.

Fontecilla-Camps JC, de Llorens R, Du MHL, Cuchillo CM. 1994. Crystal structure of ribonuclease A·d(ApTpApApG) complex. *J Biol Chem 269*:21526-21531.

Haar W, Maurer W, Rüterjans H. 1974. Proton-magnetic-resonance studies of complexes of ribonuclease A with pyrimidine and purine nucleotides. *Eur J Biochem 44*:201-211.

Hahn U, Desai-Hahn R, Rüterjans H. 1985. ^{1}H and ^{15}N investigation of the interaction of pyrimidine nucleotides with ribonuclease A. *Eur J Biochem 146*:705-712.

Hahn U, Rüterjans H. 1985. Two-dimensional ^{1}H NMR investigation of ribonuclease A and ribonuclease A-pyrimidine nucleotide complexes. *Eur J Biochem 152*:481-491.

Hirs CH, Halmann M, Kycia JH. 1965. Dinitrophenylation and inactivation of bovine pancreatic ribonuclease A. *Arch Biochem Biophys 111*:209-222.

Howlin B, Harris GW, Moss DS, Palmer RA. 1987. X-ray refinement study on the binding of cytidylic acid (2'-CMP) to ribonuclease A. *J Mol Biol 196*:159-164.

Inagaki F, Shimada I, Miyazawa T. 1985. Binding modes of inhibitors to ribonuclease T1 as studied by nuclear magnetic resonance. *Biochemistry 28*:8972-8979.

Lisgarten JN, Gupta V, Maes D, Wyns L, Zegers I, Palmer R, Dealwis CG, Aguilar CF, Hummings AM. 1993. Structure of the crystalline complex of cytidylic acid (2'-CMP) with ribonuclease at 1.6 Å resolution. *Acta Crystallogr D 49*:541-547

Lisgarten JN, Maes D, Wyns L, Aguilar CF, Palmer R. 1995. Structure of the crystalline complex of deoxycytidylyl-3',5'-guanosine (3',5'-dCpdG) cocrystallized with ribonuclease at 1.9 Å resolution. *Acta Crystallogr D 51*:767-771.

Marion D, Wüthrich K. 1983. Application of phase sensitive two-dimensional correlated spectroscopy (COSY) for measurement of proton-proton spin-spin coupling constants. *Biochem Biophys Res Commun 113*:967-974.

Meiering EM, Bycroft M, Lubienski MJ, Fersht AR. 1993. Structure and dynamics of barnase complexed with 3'-GMP studied by NMR spectroscopy. *Biochemistry 32*:10975-10987.

Neidig KP, Geyer M, Göler A, Antz C, Saffrich R, Beneicke W, Kalbitzer HR. 1995. AURELIA, a program for computer-aided analysis of multidimensional NMR spectra. *J Biomol NMR 6*:255-270.

Pavlovsky AG, Borisova SN, Borisov VV, Antonov IV, Karpeisky MY. 1978. The structure of the complex of ribonuclease S with fluoride analogue of UpA at 2.5 Å resolution. *FEBS Lett 92*:258-262.

Rance M, Sorensen OW, Baudenhausen G, Wagner G, Ernst RR, Wüthrich K. 1983. Improved spectral resolution in COSY NMR spectra of proteins via double quantum filtering. *Biochem Biophys Res Commun 117*: 479-485.

Richards FM, Wyckoff HW. 1971. Bovine pancreatic ribonuclease. In: Boyer PD, ed. *Enzymes IV*. New York: Academic Press. pp 647-806.

Rico M, Bruix M, Santoro J, González C, Neira JL, Nieto JL, Herranz J. 1989. Sequential ^{1}H-NMR assignment and solution structure of bovine pancreatic ribonuclease A. *Eur J Biochem 183*:623-638.

Rico M, Santoro J, González C, Bruix M, Neira JL, Nieto JL. 1993. Refined solution structure of bovine pancreatic ribonuclease A by ^{1}H-NMR methods. Side chain dynamics. *Appl Magn Reson 4*:385-415.

Rico M, Santoro J, González C, Bruix M, Neira JL, Nieto JL, Herranz J. 1991. 3D structure of bovine pancreatic ribonuclease A in aqueous solution: An approach to the tertiary structure determination for a small basis of ^{1}H-NMR NOE correlations. *J Biomol NMR 1*:283-298.

Robertson AD, Purisima ED, Eastman MA, Scheraga HA. 1989. Proton NMR assignments and regular backbone structure of bovine pancreatic ribonuclease A in aqueous solution. *Biochemistry 28*:5930-5938.

Santoro J, González C, Bruix M, Neira JL, Nieto JL, Herranz J, Rico M. 1993. High-resolution three-dimensional structure of ribonuclease A in solution by NMR spectroscopy. *J Mol Biol 229*:722-734.

van Gunsteren WF, Berendsen HJ. 1987. *Groningen Molecular Simulation (GROMOS) library manual*. Groningen, The Netherlands: Biomos.

Widmer H, Wüthrich K. 1986. Simulation of two-dimensional NMR experiments using numerical density matrix simulation. *J Magn Reson 70*:270-279.

Wijmenga SS, Moore MMW, Hilbers CW. 1993. NMR of nucleic acids: From spectrum to structure. In: Roberts GC, ed. *NMR in macromolecules*. Oxford: I.R.L. Press.

Wlodawer A. 1984. Structure of bovine pancreatic ribonuclease by X-ray and neutron diffraction. In: Jurnak F, McPherson A, eds. *Biological macromolecules and assemblies, vol II. Nucleic acids and interactive proteins*. New York: Wiley. pp 395-439.

Wlodawer A, Miller M, Sjölin L. 1983. Active site of RNase: Neutron diffraction study of a complex with uridine vanadate, a transition-state analog. *Proc Natl Acad Sci USA 80*:3628-3631.

Wlodawer A, Sjölin L. 1983. Structure of ribonuclease A: Results of joint neutron and X-ray refinement at 2.0 Å resolution. *Biochemistry 22*: 2710-2728.

Wlodawer A, Svensson LA, Sjölin L, Gilliland GL. 1988. Structure of phosphate-free ribonuclease A refined at 1.26 Å. *Biochemistry 27*:2705-2717.

Wodak SY, Lie MY, Wykoff HW. 1977. The structure of cytidyl (2',5') adenosine when bound to pancreatic ribonuclease S. *J Mol Biol 116*:855-875.

Wüthrich K. 1986. *NMR of proteins and nucleic acids*. New York: J. Wiley and Sons.

Zegers I, Maes D, Thi MH, Poortmans F, Palmer RA, Wyns L. 1994. The structure of RNase A complexed with 3'-CMP and d(CpA): Active site conformation and conserved water molecules. *Protein Sci 3*:2322-2339.